Study of solid molecular deuterium D_2 growth under gas pressure

S. Giusepponi, F. Buonocore, M. Celino

Italian National Agency for New Technologies, Energy and Sustainable Economic Development (ENEA) - C. R. Casaccia, Via Anguillarese 301, 00123 Rome, Italy.

M. Lupo Pasini

Computational Sciences and Engineering Division Oak Ridge National Laboratory Bldg. 5700, Rm F119, Mail Stop 6085 P.O. Box 2008, Oak Ridge, TN, 37831

A. Frattolillo

Italian National Agency for New Technologies, Energy and Sustainable Economic Development (ENEA) - C. R. Frascati, Frascati, Italy.

S. Migliori

Italian National Agency for New Technologies, Energy and Sustainable Economic Development (ENEA) - Lungotevere Thaon di Revel 76, 00196 Rome, Italy.

Abstract

The injection of high-speed cryogenic pellets made of frozen hydrogen-isotopes, represents to date the most effective method to fuel magnetically confined thermonuclear fusion plasmas. Moreover, the injection of very large pellets composed of cryogenic solid of some suitable ~~high-Z~~ impurity (typically a noble-gas such as H_2**,** Ne, or H_2/Ne, D_2/Ne mixtures), shattered in relatively small fragments just before entering the plasma, seems to be the most promising method to reduce the damage risks for the plasma-facing components in case of a plasma disruption. This technology, known as "Shattered Pellet Injection" (SPI), allows to spread out the plasma energy and mitigate possible damage to the in-vessel components, as well as to densify the plasma to suppress the formation of runaway electrons, and/or dissipate their energy. Several techniques to produce and launch cryogenic pellets have been investigated in the past decades. "Pipe gun" injectors are reliable and relatively simple devices are still commonly used today. They make use of single- or two-stage pneumatic light-gas guns to accelerate the pellet at high speeds. In these injectors, the cryogenic pellets are formed “in situ” (i.e., inside the launching barrel), by de-sublimating them directly from the gas phase, i.e., at temperatures and pressures below those of the triple point. The simplest case is pure deuterium pellets ($T < 18.7$ K, $P < 171.3$ hPa). The production of good quality solid deuterium, capable of withstanding the mechanical stress during the acceleration of the pellets, is a key issue. To this end the phase transition of deuterium from gas to solid (and vice versa) is modeled with extensive molecular-dynamics (MD) simulations. Moreover, the solid growth from the gas phase is simulated in an ample range of temperatures and pressures, to find the best compromise between growth velocity and mechanical properties of the resulting solid system.

1. Introduction

Contemporary magnetically confined D/D nuclear fusion experiments require a flexible fueling system, including both gas-puffing and pellet injection. To sustain the core plasma density, cryogenic deuterium pellets of appropriate size, typically in the order of a few mm (corresponding to a suitable fraction of the total plasma particles content), must be injected at sufficiently high speed to penetrate

and release the fresh fuel deeply inside the plasma column. The injection velocity needed for an effective core fueling depends on the density and temperature profiles of the target plasma, on the pellet mass, as well as, in the case of a tokamak configuration, on the injection location. In a tokamak, indeed, the fuel deposition depth results from two distinct phenomena, namely: the pellet penetration (i.e., the distance traveled by the pellet until it is completely ablated by the plasma), followed by the drift of the locally ablated diamagnetic cloud in the direction opposite to the gradient of the magnetic field [1]. For a given target plasma, the pellet penetration increases with its mass and speed; in present day tokamaks it may be larger than the drift displacement, and hence contribute substantially to the fuel deposition depth [1]. Injection from the High Field Side (HFS) can take advantage of the outward drift effect, thus requiring lower pellet velocities than those used in the injection from the Low Field Side (LFS) [2, 3]. However, the implementation of HFS fueling schemes results in a greater complexity of the Pellet Injection System (PIS), demanding the introduction of transfer systems capable of redirecting the pellets delivered by the launcher to their inboard injection location. Inside such transfer systems, the pellets are constrained to move along a guiding track, featuring several bends with different curvature radii, where they undergo centrifugal stress and partially vaporize, often giving rise to an undesired pressure buildup [4, 5]. Moreover, due to the poor mechanical properties of the solid deuterium, the centrifugal stress (which is proportional to the square of the pellet velocity and inversely proportional to the local curvature radius of the track) may result in breaking the cryogenic projectiles, thus severely limiting the transfer speed. Lacking a proper model, an empirical scaling law, calibrated on the AUG experiment for cubic shaped D_2 pellets, is commonly adopted [6] to estimate the maximum speed V_{inj} (m/s) that pellets can withstand, given the local curvature radius R(m) of the guide tube, and the pellet size L(m):

$$V_{inj}(m/s) = 36.4\sqrt{R/L}$$

Next step large D/T fusion devices, like the International Thermonuclear Experimental Reactor (ITER) and the DEMOnstration Fusion Reactor (DEMO), will require either D_2 or mixed D/T fuel pellets of correspondingly larger size, likely to be injected at relatively higher speeds. In ITER, as well as in future fusion reactors, plasma disruptions may result in considerable damages of the material surfaces of the plasma facing components, such as the first wall and the divertor, due to the intense heat flux generated by the rapid and local deposition of the plasma energy, and to the large currents of high-energy runaway electrons produced during the plasma current quench. Moreover, the strong halo currents generated when the plasma strikes the wall, result in very large mechanical loads that can harm not only the first wall, but also the underlying support structures. All these detrimental effects contribute to severely limit the lifetime of the reactor and require identification of adequate strategies to prevent disruptions [7, 8]. However, some disruption may occur anyway, therefore suitable

disruption mitigation tools need to be developed. To date, the most promising method to attenuate the undesired effects of plasma disruptions consists in the injection of very large, high-speed impurity pellets (H_2, Ne or H_2/Ne, D_2/Ne mixtures) to produce strong radiation, which dumps the plasma energy quickly but uniformly on the first wall and provides collisional suppression of runaway electrons. The main advantage of using cryogenic solids is that the material turns to gas and can be easily pumped out after usage. Very large impurity pellets are needed to get the density high enough to prevent the onset of runaway electrons. Such big pellets, if injected intact, would likely not ablate completely within the plasma, due to their large mass. They might therefore partially survive across the plasma and hit the wall on the opposite side with sufficient kinetic energy to potentially damage the first wall materials themselves [9]. To avoid this issue, as well as to better assimilate the injected material into the plasma [10], the pellets are purposely shattered in small (much less penetrating) fragments by impact inside a bent tube or against a metal target plate, just before entering the disrupting plasma. For this reason, this technique is known as "Shattered Pellet Injection" (SPI) [11].

The formation of large (15 to 30 mm) pure or mixed pellets is rather challenging, due to the relatively poor thermal conductivity of the solid material that prevents sufficiently quick removal of the latent heat during the de-sublimation process as the solid layer becomes more and more thick. This slow heat removal may result in a rather long time to form a pellet [12]. As for fueling, the rather poor mechanical properties of solid hydrogen isotopes require accurate control of pellet formation to produce solid deuterium of the best possible quality, in order the pellets can withstand the huge mechanical stress they undergo during acceleration to high speeds, as well as the centrifugal stress inside curved guiding transfer systems. Exploring the phase transition of deuterium from gas to solid (and vice versa) by extensive molecular-dynamic (MD) simulations, represents a valid support to investigate the mechanical properties of the resulting solid, as well as to optimize the de-sublimation parameters. The computational details and results of this study are reported in this paper. As a next step, we plan to use the same method to extend the analysis to the case of cryogenic pellets made of noble gases (H_2, Ne) or gas mixtures, such as H_2/Ne, D_2/Ne or D/T.

To describe and characterize the growth process of the pellets by solidification of gaseous deuterium, it is necessary to explore the phase transition at temperatures and pressures below the triple point: T = 18.7 K, P = 172 mbar [13, 14]. Since hundreds of thousands of molecules are needed to accurately model the entire phase transition process, classical molecular dynamics methods are used (section 2). We investigated the de-sublimation process in which molecules of gaseous deuterium, at 25 mbar, solidify on a cold surface, and characterized the resulting solid to compare its properties with experimental results reported in literature [15]. We also calculated the absorption rate and the equilibrium temperature. Moreover, slab and surface are characterized in terms of the separation

between initial and reconstructed solid slabs, the smoothness of its free surfaces, and the percentage of particle in FCC lattice positions. This can provide useful insights on the experimental parameters to improve the quality of solid deuterium. The deuterium crystalline phase, its free surface, and the gas phase are investigated as three separate systems (one-phase systems), before simulating the gas/solid interface (two-phase system). In the next section the computational details used for the MD simulations of the deuterium one-phase systems are presented. Then, in section 3, results from deuterium two-phase system are shown and discussed.

2. Computational details

The LAMMPS (Large-scale Atomic/Molecular Massively Parallel Simulator) code is used to perform MD simulations of the molecular deuterium (D_2) systems. LAMMPS is a classical MD code that models particles ensembles in solid, liquid or gaseous state to address atomic, polymeric, biological, metallic, granular, and coarse-grained systems by using a variety of force fields and boundary conditions [16, 17].

Both one-phase and two-phases systems have been simulated in a temperature range spanning from the absolute zero temperature (T = 0 K) up to temperatures and pressures near the D_2 triple point. To perform constant pressure and temperature MD (NPT-MD), both pressure and temperature are controlled by the Berendsen barostat and thermostat [18]. A timestep as small as t_s = 0.001 ps is implemented to accurately integrate equations of motion at all temperatures. Given the scope of the paper and the errors (less than 6%) among experimental and computational estimates of quantities of interest in this work, we resorted to a classical Lennard-Jones potential to model interactions between particles. More accurate estimates can be achieved exploiting interatomic potentials that are already available in literature [19, 20]. The Lennard-Jones potential is implemented with ε = 2.29 meV and σ = 3.07 Å (cutoff of 3.5σ ~ 10 Å) as reported in Ref. [20]. Periodic Boundary Conditions (PBC) were imposed to mimic an infinitely extended system in x, y and z directions.

The crystal atomic structure of solid deuterium is still an open field of research in the scientific literature; in the low temperature part of its phase diagram, both face centered cubic (FCC) and hexagonal close packed (HCP) structures are supposed to form, depending on the preparation conditions. However, the FCC structure seems to be the most likely at low pressure and low temperature. The experimental FCC lattice parameter is estimated to be a_{D2} = 5.07 ± 0.05 Å considering reflection and transmission diffraction patterns obtained from thin films of solid deuterium at about 5 and 7 K [21].

Considering the D_2 molecule as a single particle, the numerical model is composed by N = 64000 D_2 particles forming a crystalline FCC bulk (40 × 40 × 10 crystal unit cells) representing a 128000 deuterium atoms system. By performing the energy minimization at T = 0 K, the lattice parameter

and the cohesion energy of the numerical model are found to be a_0 = 4.75 Å and E_{coes} = 19 meV/particle, respectively (tetragonal simulation cell, 190 Å × 190 Å × 47.5 Å).

In order to characterize the crystalline phase model, the system is heated from the absolute zero temperature up to 30 K (in step of 1 K) in which it is surely melted. Every MD simulation, at constant pressure P = 0 mbar, simulates 1000 ps: the first 200 ps are used to raise (1 K) the temperature of the system, the next 800 ps are used to stabilize it at the new temperature. Physical quantities are computed averaging over the last 500 ps of simulation, to ensure that the systems have reached their equilibrium and provide sufficiently accurate estimates. This procedure gives an estimate of the mechanical melting temperature that is found to occur between 20 and 21 K at zero external pressure. As expected, the melting temperature is higher than the experimental one because the solid is heated uniformly till the complete melting. Though the atomistic model is based on a very simple interatomic scheme, the computed heat of fusion ~~is~~ H_f = 250.5 J/mol has the same order of magnitude as the experimental one (199 J/mol Ref. [14]).

The same thermal treatment is adopted to characterize the solid D_2 surface. The surface is yield cutting the previous relaxed solid at zero temperature along the (001) Miller plane and extending the simulation cell orthogonally to the surface (L_z = 200 Å) to have a void region of about 150 Å on it. PBC are imposed along x and y directions to have an infinitely solid slab with two free surfaces perpendicular to the z direction.

The gas phase is prepared starting from N = 64000 D_2 particles randomly placed in a tetragonal simulation cell with: $L_x = L_y$ = 190 Å and L_z derived from the ideal gas equation with T = 30 K and P = 25 mbar. The gas system is equilibrated for 1000 ps by NPT-MD, in which $L_x = L_y$ are kept fixed, and L_z is free to vary. The final configuration is used as starting configuration for the cooling process of the gas in which the temperature is decreased down to 5 K (in step of 1 K) by performing MD simulations at constant pressure P = 25 mbar. As already done for the bulk solid and the surface, each run lasts 1000 ps, where 200 ps are used to lower the temperature by 1 K and the successive 800 ps are used to thermalize the system. The statistical analysis, performed on the last 500 ps, confirms that all the simulated systems are always well equilibrated.

The solid-gas deuterium interfaces in the range of temperature T = 5 - 20 K are formed by coupling the D_2(100) surface and the gas systems previously prepared. The starting configurations are composed by a slab of solid deuterium that exposes two free surfaces (orthogonal to the z direction) to a gas of deuterium at initial distance of 100 Å to permit both systems to interact gradually. The systems are infinitely extended in the x and y directions thanks to PBC. An external pressure of 25 mbar is applied on the gas to better reproduce experimental conditions [15].

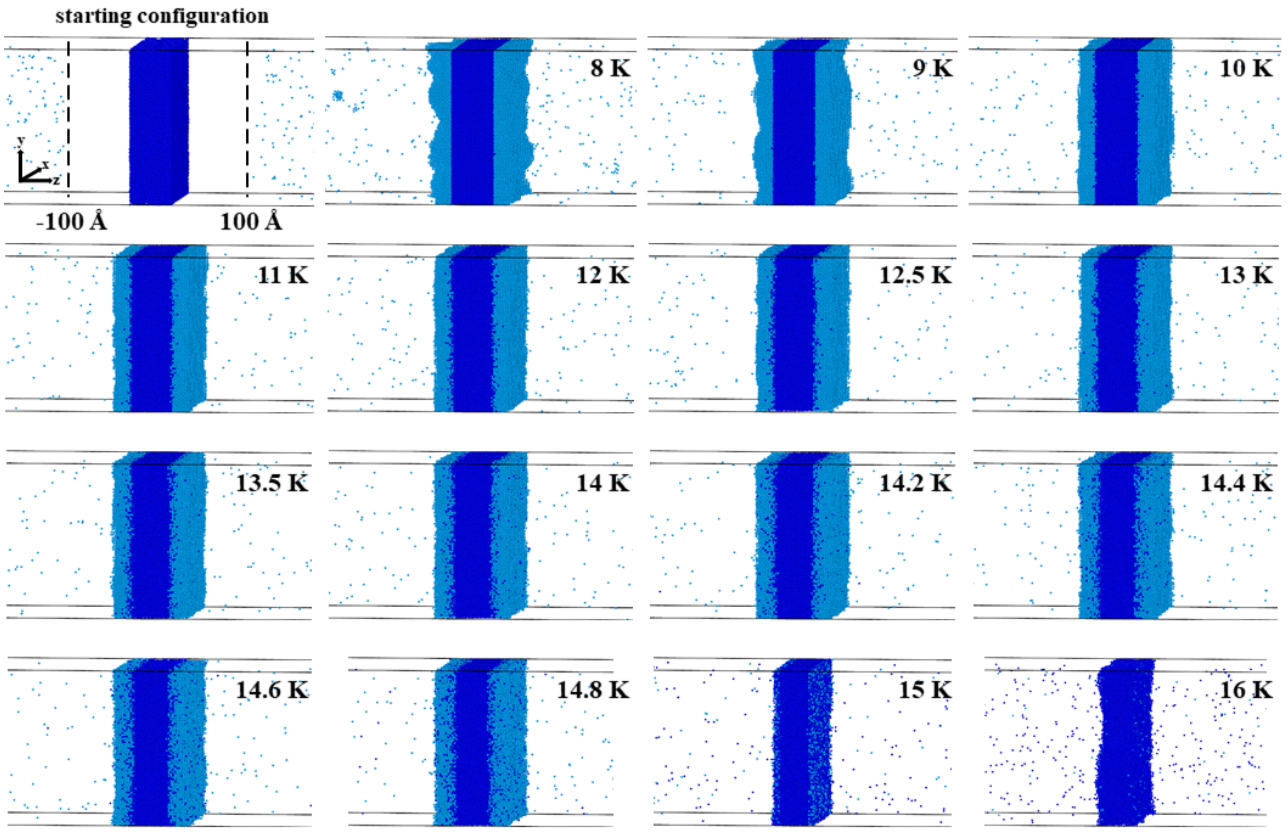

***Figure 1**. Starting and reconstructed configurations after the +75% increase of solid phase in the temperature range T = 8 - 14.8 K. Snapshots of solid deuterium slab in sublimation regime at T = 15 K and T = 16 K, respectively. Dark blue spheres are particles that initially were in solid phase, whereas light blue spheres are those initially in gas phase.*

3. Results and discussion

Cryogenic pellets are formed by solidifying gaseous deuterium at a constant pressure, below that of the triple point. The evolution of the two-phases system, starting from the configuration shown in the upper left corner of Figure 1, with an imposed pressure of 25 mbar in the z direction and 0 mbar in the x and y directions, has been investigated by performing a set of MD simulations for different values of the temperature T, in the range of 5 to 20 K (in step of 1 K). This study reveals that, for T < 15 K, de-sublimation is favored, and the solid phase grows at a rate that decreases with the temperature, whereas, for T ≥ 15 K, sublimation prevails and the solid phase decreases. Then, we can infer that the equilibrium condition at P = 25 mbar occurs within the temperature range T = 14 - 15 K. In order to have a better estimate of the temperature of the equilibrium condition, other MD simulations were performed at T = 12.5, 13.5, 14.2, 14.4, 14.6 and 14.8 K.

Simulations in the temperature range from 8 up to 14,8 K are all ended when a 75% increase of the solid phase, with respect to the starting configuration, is achieved (from 64000 up to 112000 D_2

molecules). For the simulations outside that temperature range, we do not define a limit in terms of number particles in solid phase, because for T < 8 K the system collapses to the solid phase, whereas, for T ≥ 15 K, is the number of particles in gaseous phase that increases.

Slabs in Figure 1 show that for low and high T the final surfaces are more corrugated than surfaces at intermediated temperatures. Both low and high temperatures for different reasons do not allow the reconstruction of ordered surfaces. This is clearly seen in both the T = 8 K and T = 14.8 K configurations in Figure 1. It can be expected that at very low temperatures, already in gaseous phase, there is the tendency of the particles to freeze quickly with the formation of clusters (see panel 8 K in Figure 1) that dropping on the solid slab remain stuck on it giving rise to a corrugated surface. Then, this could be an indicator that a too fast solidification gives rise to the formation of a sort of "snow" rather than "ice". On the contrary, at higher temperature the sublimation process begins to be competitive with that of de-sublimation. It is conceivable that at the separation surface between the solid and the gas there is a continuous exchange of particles between the two phases, which does not favor the formation of a regular and well-ordered surface (see panel 14.8 K in Figure 1). This is also confirmed considering the mixing between dark and light blue spheres in the snapshots (dark blue spheres are particles that initially were in solid phase, whereas light blue spheres are those initially in gas phase).

In order to characterize the sublimation/de-sublimation process and quantify the corresponding rates, in Figure 2a we report, for each T, the number of particles in the solid phase during the MD simulation. The first result is that if T < 8 K the system collapses quickly to a solid phase, whereas for T > 15 K sublimation to gas phase is observed; therefore, the growth of the solid phase is expected to occur in the temperature range T = 8 - 15 K. Moreover, no intermediate transition to the liquid phase is observed in the MD simulations, in agreement with the experimental observation that, in these thermodynamical conditions, there is only coexistence of solid and gas phases. Numerically, solid, liquid and gaseous phases are easily identified by combining several quantities: particle potential energies, local symmetries and radial pair correlation functions.

We observe in Figure 2a that, after a short initial transient, the number of solid particles increases almost linearly with time during the simulation. Moreover, as T increases to approach T_e, the slope of the curves diminishes, approaching zero for the equilibrium condition. For T ≥ 15 K, the desorption process is favored, and the number of solid particles decreases in time. Thus, a good estimate of the equilibrium condition temperature is $T_e \cong 14.9$ K. In Figure 2b the time required to increase the number of solid D_2 particles from 64000 up to 80000 (+25%; red symbols), 96000 (+50% green symbols) and 112000 (+75% blue symbols) is reported as a function of the temperature; these curves show an almost linear increase with the temperature up to about 13 K, followed by a sharp increase

of their slope as T approaches T_e, indicating a sudden decrease of the solidification rate. Therefore, T = 13 K could be considered a superior limit to the linear behavior and represents the highest T to have good solidification rates.

In Figure 2c the experimental solid-gas coexistence curve is reported (red crosses) to estimate the equilibrium temperature at P = 25 mbar, which corresponds to $T_e \cong 15.5$ K. In Figure 2c the numerical results are also reported: if T < 14.9 K (blue symbols) the system tends to be solid, if T > 14.9 K (green) the system tends to evolve to the gas phase, in very good agreement with the experimental findings [13, 15].

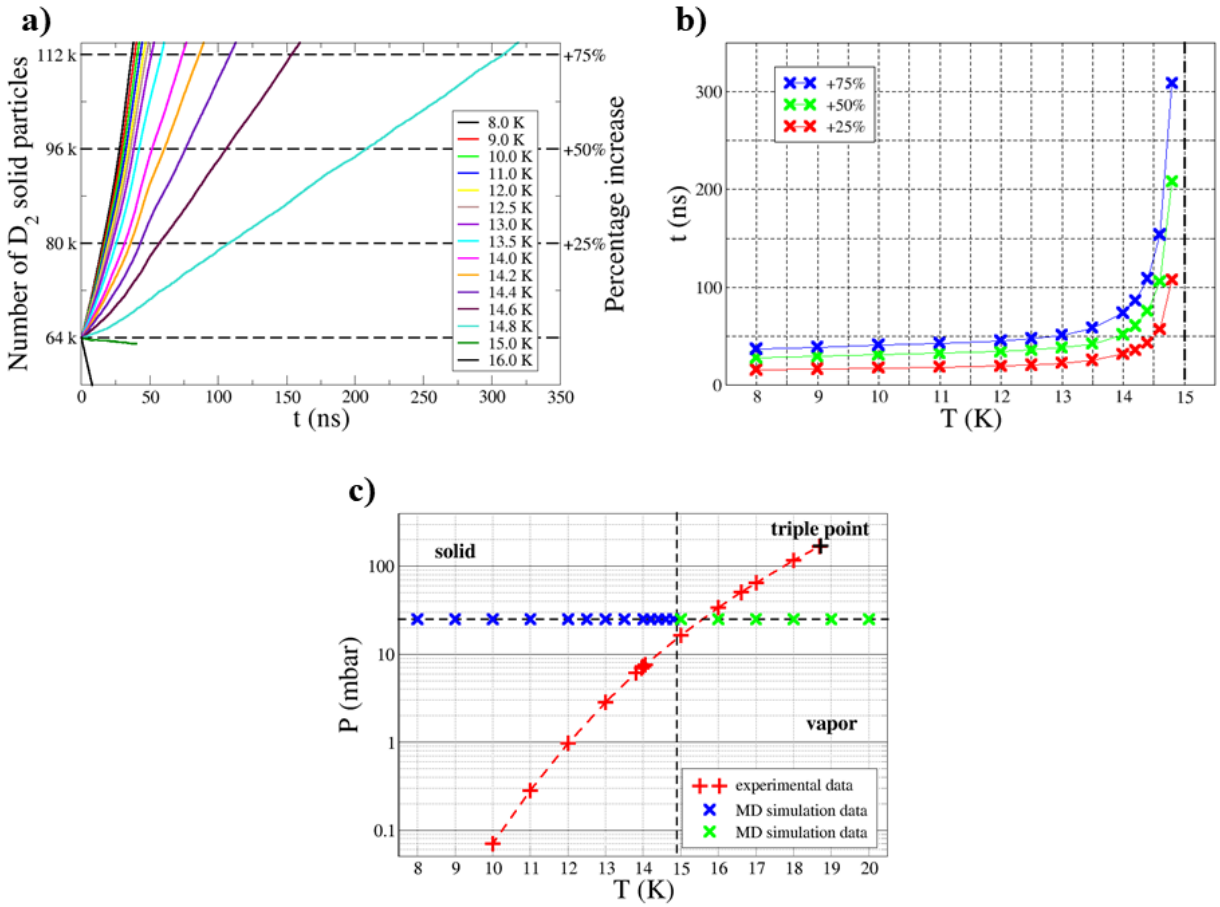

***Figure 2**. a) Number of D_2 particles in the solid phase during the MD simulations in the temperature range T = 8 - 16 K. On the left vertical axis, the number of particles in the solid phase is reported. On the right vertical axis, the percentage increase of particles with respect to the starting configuration is reported. The lower is T, the higher is the rate of solid growth. b) Time required to increase the number of D_2 particles in solid phase from 64000 up to 80000 (+25% red symbols), 96000 (+50% green symbols) and 112000 (+75% blue symbols), respectively, in the temperature range T = 8 - 14.8 K. c) Red symbols are the experimental solid-vapor equilibrium curve [13, 15] in which the last point is the D_2 triple point (black symbol). Blue/green symbols are the MD simulations*

in the solid/gas phase. The numerical estimation of the solid-vapor equilibrium temperature ($T_e \cong 14.9$ K) is in good agreement with the experimental value ($T_e \cong 15.5$ K).

In Figure 3a the ratio A/A_0 is plotted versus temperature, to compare the area A of the free surface of the reconstructed slabs and the free surface area A_0 of the initial slab [22, 23] (see surfaces in Figure 1). We can distinguish two different trends: in the T < 10 K range, the ratio decreases very fast with increasing T, until a minimum is reached, while in the T > 10 K range the ratio A/A_0 increases almost linearly with T. This linear behaviour enhances as the equilibrium temperature is approached. These findings reflect the fact that for low T the particles freeze quickly, as observed before, giving rise to very corrugated surfaces, while for high temperature the particles have increased mobility between the solid and the gas phases, resulting in a more "fluid" solid with a wavy surface. In addition, we report this ratio at different level of growth of the solid slab: red curve/symbols refer to +25%, green curve/symbols refer to +50% and blue curve/symbols refer to +75%. The two trends previously described are still present, however, it is interesting to note that the curves intersect at about T = 10 K. Then, for T < 10 K, the growth of the solid is combined with a pronounced increase of the surface irregularities (the lower the temperature, the more evident this phenomenon is). On the contrary, for T > 10 K, the growth of the solid is characterized by a lower roughness of the surface. To further characterize the roughness of the reconstructed surfaces we consider the distribution of the solid particles along the z direction (at +75%) as shown in Figure 3b. In the graphs we report the number of solid particles versus their z coordinate in the temperature range T = 8 - 14.8 K with respect to the ideal case of the step function. At T = 8 K there is the maximum spread of the particle position along z direction. As the temperature increases, the curves approach the step function up to 10 - 11 K, after which there is a trend reversal in which the surfaces become more and more wavy up to 14.8 K.

To identify the FCC crystal structure, we inspected the local structural environment of the atoms using the adaptive common neighbour analysis (a-CNA) [22, 24]. In Figure 3c, the percentage of solid particles occupying FCC lattice positions is plotted versus the temperature T: this percentage is about 90% for T < 12 K (with a maximum in the 9 to 10 K range) and decreases to ~ 70% as T approaches T_e. Therefore, the solid particles are more likely to be found in the stable FCC lattice for T < 12 K. We also checked the fraction of solid particles in the FCC lattice positions for different levels of solid phase growth (25%, 50% and 75%), but no difference was found in this case.

Finally, a further set of MD simulations was performed to evaluate the influence of the gas pressure on the de-sublimation rate. We fixed the temperature at T = 12 K and allowed the pressure to vary the range 15 – 50 mbar, in steps of 5 mbar. As before, the rate was estimated by the time t required to achieve a +75% increment of particles in the solid phase. This time t turns out to be inversely proportional to P, as shown in Figure 3d. This behaviour can be explained considering the ideal gas

law. The increment of solid phase causes a reduction of the number of particles in the gas phase resulting, at constant temperature, in a contraction of the gas volume $L_x \times L_y \times L_z$, which is inversely proportional to the pressure; since, in our case, L_x and L_y remain almost constant, L_z is proportional to 1/P. On the other hand, the average speed <v> of the gas particles, according to the Maxwell's distribution, does not depend on the pressure, so that the average time <t> required to travel the distance L_z, is proportional to L_z, resulting in the predicted inverse proportionality between the time t and the pressure P.

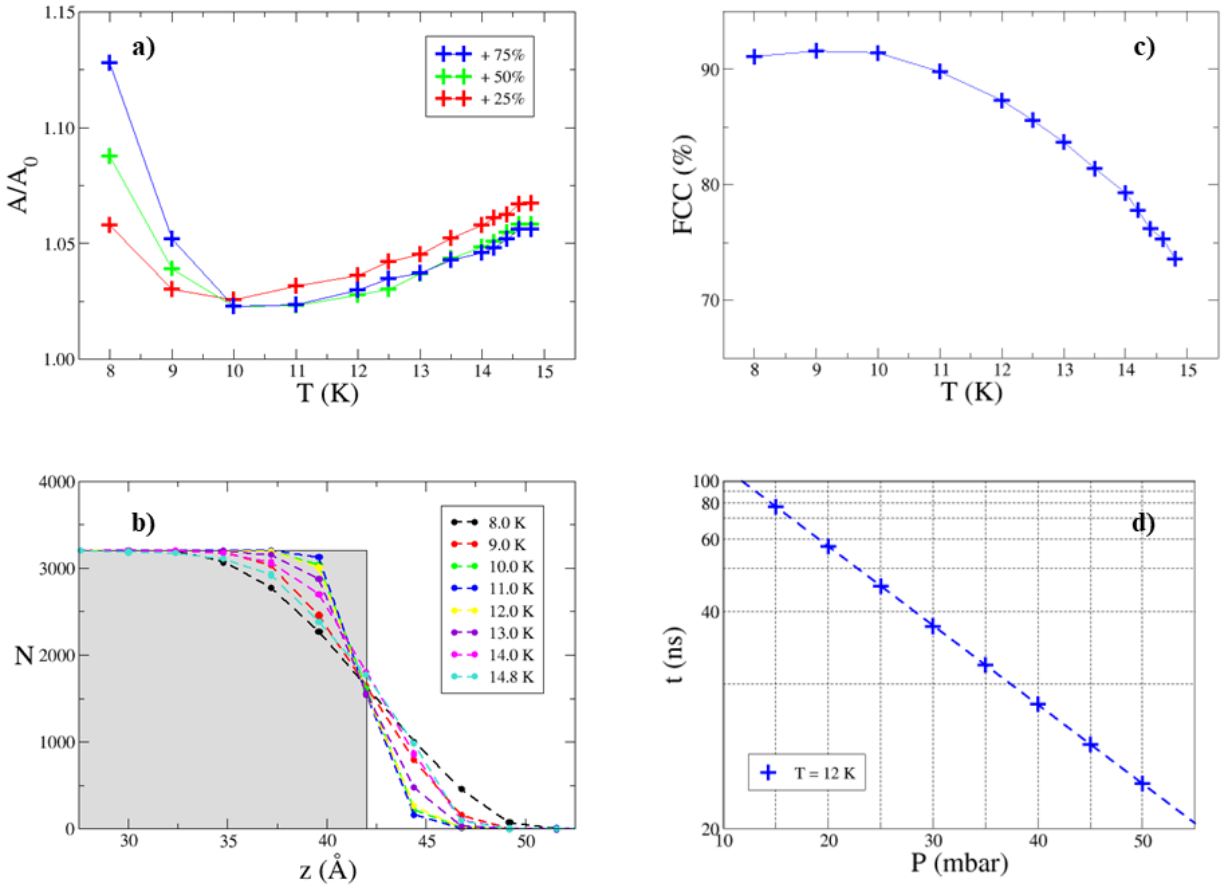

Figure 3. *a) A/A_0 ratio plotted versus temperature. A_0 is the free surface area of the slab in the initial configuration, A is the free surface area of the reconstructed slab at different percentage of increasing: +25% red curve/symbols; +50% green curve/symbols; +75% blue curve/symbols. b) Number of solid deuterium particles vs. their position z for the configurations after the +75% increase of solid phase in the temperature range T = 8 - 14.8 K. Shadow gray area refers to the step function ideal case. c) Percentage of particles in FCC lattice positions after a 75% increase of solid phase. d) Time required to increase the number of D_2 particles in solid phase by 75% of the initial value, versus pressure in the range 15 – 50 mbar, at fixed temperature T = 12 K.*

Conclusions

This work clearly shows that the coexistence of solid and gaseous deuterium system can be simulated in a surprisingly reliable way, rich of interesting physics, using a simple atomistic numerical model. The chosen numerical model turns out that it can provide a meaningful description of the sublimation/de-sublimation process as a function of its thermodynamic parameters, can predict the equilibrium temperature (for a given constant pressure) and the solid lattice parameters, in quite good agreement with experimental values reported in literature. Moreover, the reconstructed solid slabs are analyzed and characterized in order to have insights about the conditions for the formation of high-quality pellets.

The study presented in this paper is mainly focused on a 25 mbar pressure system since this is a typical value to form pellets in a pipe-gun injector. The developed numerical procedure can be extended to other pressures below the triple point. Our numerical method provides useful indications to optimize the formation parameters of D_2 pellet and to identify, for a given pressure, the optimum temperature range allowing to speed-up the process as much as possible (which is particularly important for very large pellets), while ensuring the production of a solid featuring sufficiently good quality to withstand the huge stress during acceleration. The simulations reveal that there is a range of temperatures around T = 12 K in which a good compromise can be found, indeed:

- For low and high temperatures, the final surfaces are more corrugated than surfaces at intermediated temperatures.
- $T < 13$ K the reconstruction rate is high, at higher T it slows down very quickly. So, T = 13 K can be considered a superior limit to have good solidification rates
- In the range $10 K < T < 13 K$ the reconstructed surfaces approach to a smooth shape.
- For $T < 13$ K the reconstructed slabs are the most ordered.

We plan, soon, to extend this method to other pressure range for Deuterium and other gases of interest for fusion applications, such as Hydrogen, Neon, and to gas mixture of these elements.

Acknowledgments

Part of this research benefited of the user grant support delivered by the Center for Nanophase Materials Sciences (CNMS) of Oak Ridge National Laboratories (USA). This research used resources of the National Energy Research Scientific Computing Center (NERSC), a U.S. Department of Energy Office of Science User Facility located at Lawrence Berkeley National Laboratory, operated

under Contract No. DE-AC02-05CH11231. The computing resources and the related technical support used for this work have been provided by CRESCO/ENEAGRID High Performance Computing infrastructure and its staff [25]. CRESCO/ENEAGRID High Performance Computing infrastructure is funded by ENEA, the Italian National Agency for New Technologies, Energy and Sustainable Economic Development and by Italian and European research projects, see http://www.cresco.enea.it/english for information. The authors acknowledge the extensive use of the ENEA FARO facility and the support of its management team [26].

Bibliography

1) B. Pégourié, Ch. Day, A. Frattolillo, F. Koechl and P.T. Lang. 2016 Physical constraints on the design of the DEMO pellet fueling system. *Proc. of the 43rd EPS Conf. on Plasma Phys.* Leuven (B) P4.076.
2) P. T. Lang *et al*. 1997 High-Efficiency Plasma Refuelling by Pellet Injection from the Magnetic High-Field Side into ASDEX Upgrade. *Phys. Rev. Lett.* **79** 1487.
3) L. R. Baylor *et al*. 2007 Comparison of deuterium pellet injection from different locations on the DIII-D tokamak. *Nucl. Fusion* **47** 1598-1606.
4) S.K. Combs *et al*. 2005 Pellet delivery and survivability through curved guide tubes for fusion fueling and its implications for ITER. *Fus. Eng. Design* **75-79** 691-696.
5) A. Lorenz *et al*. 2003 Mass transfer in long pellet guiding systems at ASDEX upgrade and JET. *Fus. Eng. Design* **69** 15-20.
6) P. T. Lang, Ch. Day, E. Fable, Y. Igitkhanov, F. Köchl, R. Mooney, B. Pégourié, B. Ploeckl, R. Wenninger and H. Zhom. 2015 Considerations on the DEMO pellet fueling system. *Fus. Eng. Design* **96-97** 123-128.
7) G. Pautasso *et al*. 2002 On-line prediction and mitigation of disruptions in ASDEX Upgrade. *Nucl. Fusion* **42** 100.
8) B. Cannas, A. Fanni, E. Marongiu, and P. Sonato. 2004 Disruption forecasting at JET using neural networks. *Nucl. Fusion* **44** 68.
9) S. K. Combs *et al*. 2010 Alternative techniques for injecting massive quantities of has for plasma-disruption mitigation. *IEEE Trans. Plasma Sci.* **38** 400-405.
10) L. R. Baylor *et al*. 2009 Pellet fuelling, ELM pacing and disruption mitigation technology development for ITER. *Nucl. Fusion* **49** 085013.
11) T. E. Gebhart *et al.* 2021 Recent progress in shattered pellet injection technology in support of the ITER disruption mitigation system. *Nucl. Fusion* **61** 106007.

12) L. R. Baylor *et al*. 2019 Shattered pellet injection technology design and characterization for disruption mitigation experiments. *Nucl. Fusion* **59** 066008.
13) P. C. Souers. 1986 Hydrogen Properties for Fusion Energy. *University of California Press*, Berkley and Los Angeles, California.
14) F. Pavese and C. Barbero. 1979 The triple point of pure normal deuterium. *Cryogenics* **19** 255.
15) S. K. Combs, L. R. Baylor, C. R. Foust, A. Frattolillo, M. S. Lyttle, S. J. Meitner and S. Migliori. 2015 Experimental Study of the Propellant Gas Load Required for Pellet Injection with ITER-Relevant Operating Parameters. *Fusion Sci. Technol.* **68** 319-325.
16) S. Plimpton. 1995 Fast parallel algorithms for short-range molecular dynamics. *J. Comp. Phys.* **177** 1-19.
17) https://lammps.sandia.gov/
18) H. J. C. Berendsen, J. P. M. Postma, W. F. van Gunsteren, A. Di Nola and J. R. Haak. 1984 Molecular dynamics with coupling to an external bath. *J. Chem. Phys.* **81** 3684.
19) I. F. Silvera and V. V. Goldman. 1978 The isotropic intermolecular potential for H_2 and D_2 in the solid and gas phases. *J. Chem. Phys.* **69** 4209.
20) L. A. Zepeda-Ruiz, B. Sadigh, S. J. Shin, B. J. Kozioziemski and A. A. Chernov. 2018 Effect of wetting on nucleation and growth of D2 in confinement. *J. Chem. Phys.* **148** 134708.
21) A. E. Curzon and A. J. Mascall. 1965 The crystal structures of solid hydrogen and solid deuterium in thin films. *Brit. J. Appl. Phys.* **16** 1301.
22) A. Stukowski. 2010 Visualization and analysis of atomistic simulation data with OVITO - the Open Visualization Tool. *Modell. Simul. Mater. Sci. Eng.* **18** 015012.
23) A. Stukowski. 2014 Computational Analysis Methods in Atomistic Modeling of Crystals. *JOM* **66** 399-407.
24) A. Stukowski. 2012 Structure identification methods for atomistic simulations of crystalline materials. *Modell. Simul. Mater. Sci. Eng.* **20** 045021.
25) F. Iannone *et al*. 2019 CRESCO ENEA HPC clusters: a working example of a multifabric GPFS Spectrum Scale layout. 2019 *International Conference on High Performance Computing & Simulation (HPCS)*, Dublin, Ireland, 1051-1052.
26) A. Mariano, G. D'Amato, F. Ambrosino, G. Aprea, F. Buonocore, M. Celino, A. Colavincenzo, M. Fina, A. Funel, S. Giusepponi, G. Guarnieri, F. Palombi, S. Pierattini, G. Ponti, G. Santomauro, G. Bracco and S. Migliori. 2019 Fast Access to Remote Objects 2.0. A renewed gateway to ENEAGRID distributed computing resources. *FGCS* **94** 920-928.